National Renewable Energy Laboratory

Innovation for Our Energy Future

Polymer Hybrid Photovoltaics for Inexpensive Electricity Generation

Final Technical Report
1 September 2001 — 30 April 2006

S.A. Carter
University of California–Santa Cruz
Santa Cruz, California

Polymer Hybrid Photovoltaics for Inexpensive Electricity Generation

Final Technical Report
1 September 2001 — 30 April 2006
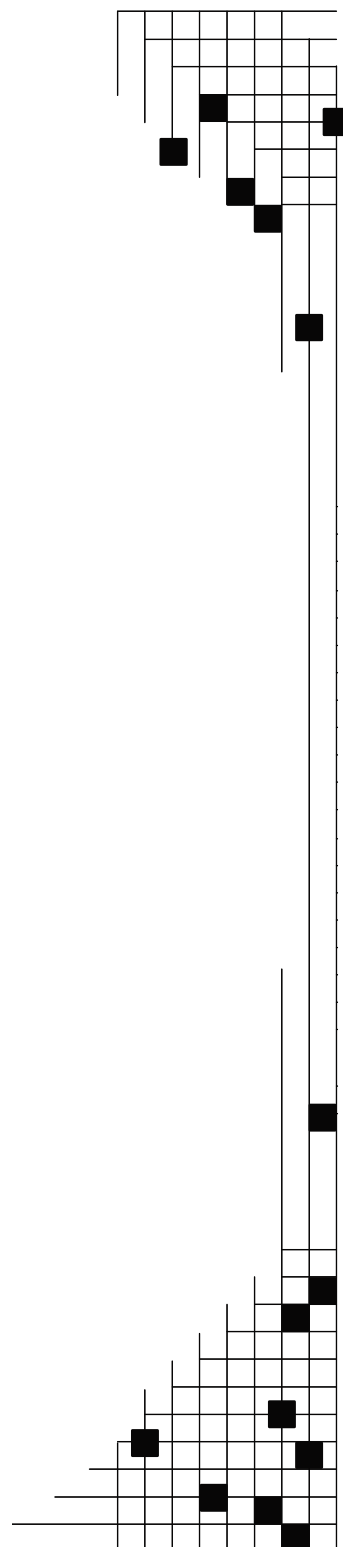
S.A. Carter
University of California–Santa Cruz
Santa Cruz, California

NREL Technical Monitors: R. McConnell, F. Posey-Eddy

Available electronically at http://www.osti.gov/bridge

Available for a processing fee to U.S. Department of Energy
and its contractors, in paper, from:
     U.S. Department of Energy
     Office of Scientific and Technical Information
     P.O. Box 62
     Oak Ridge, TN 37831-0062
     phone: 865.576.8401
     fax: 865.576.5728
     email: mailto:reports@adonis.osti.gov

Available for sale to the public, in paper, from:
     U.S. Department of Commerce
     National Technical Information Service
     5285 Port Royal Road
     Springfield, VA 22161
     phone: 800.553.6847
     fax: 703.605.6900
     email: orders@ntis.fedworld.gov
     online ordering: http://www.ntis.gov/ordering.htm

Printed on paper containing at least 50% wastepaper, including 20% postconsumer waste

Table of Contents

List of Figures

List of Tables

Project Objective: The project goal is to understand the operating mechanisms underlying the performance of polymer hybrid photovoltaics to enable the development of a photovoltaic with a maximum power conversion efficiency over cost ratio that is significantly greater than current PV technologies. Plastic or polymer-based photovoltaics can have significant cost advantages over conventional technologies in that they are compatible with liquid-based plastic processing and can be assembled onto plastic under atmospheric conditions (ambient temperature and pressure) using standard printing technologies, such as reel-to-reel and screen printing. Moreover, polymer-based PVs are light weight, flexible, and largely unbreakable which make shipping, installation and maintenance simpler.

Executive Summary of Project Results: This final report summarizes the research completed by Sue Carter's group in the physics department at the University of California, Santa Cruz. Major collaborators included J. Campbell Scott at IBM Almaden Research Center, Garry Rumbles at the National Renewable Energy Laboratories, Melissa Kreger at Add-vision, and H. Horhold at the University of Jena, Germany. This research comprises the PhD dissertations of Yuko Nakazawa and Stephanie Chasteen who were both supported under this contract. This contract also supported Melissa Kreger while she was postdoctoral researcher in Carter's laboratory. In addition, several undergraduate students, including Tosan Ombegedho, Peter Journey-Kaler, Gareth Fortser, Charles Dearie, and Samuel Bergenher completed research on this contract. The contract resulted in six publications currently published or in press, and another two publications that are in the final process of submission. Furthermore, a numerical simulation program was developed (in collaboration with IBM) to fully simulate the performance of multicomponent polymer photovoltaic devices, and a manufacturing method was developed (in collaboration with Add-vision) to inexpensively manufacture larger area devices.

The research completed under this contract included research into higher conversion efficiency polymer photovoltaics that maintained longer lifetime and reliability with an inexpensive manufacturing process. Studies were completed on novel PPV and polythiophene-based hole transporting polymers blended or layered with electron transporting polymers, such as CN-ether-PPV, as well as TiO_x, and C_{60}-based nanoparticles. Blends with semiconducting nanoparticles were also studied; however, these experiments were not completed by the end of the contract. Several different polymer hole transport materials were developed and characterized in an attempt to improve charge transport and increase absorption across visible spectrum. The use of different electrode geometries and tandem structures to improve device efficiency was evaluated. Different TiO_x, and C_{60}-based morphologies were tested to understand their impact on charge dissociation and transportation. The completed characterization studies on the three main classes of photovoltaic devices included temperature dependence of PV device performance, dependence of device performance and degradation on operation conditions and device morphology, evaluation of the how the device performance depends on excited state dynamics through steady state and time resolved photoluminescence measurements (in collaboration with NREL), numerical simulations of device performance (in collaboration with IBM), and the viability of manufacturing the structures using a low cost printing process (in collaboration with Add-vision).

The main outcome and conclusions of these results are:
• Polymer/PCBM (i.e. C_{60}) blends resulted, as expected, in the highest power conversion efficiency (~4%) of all device structures studied due to greater mobility of C_{60}. Much greater

power conversion efficiencies can be expected in this system through optimization of blend/layer morphology.
• Exciton dissociation is insufficient for optimization of device performance. Improved exciton generation rate, through the presence of exciplexes, or layer thickness control, and charge transport pose more important limitations to performance.
• Emissive interchain excitations may serve as useful sources of separable charge, whereas poorly emissive single-chain excitations are difficult to quench due to competing non-radiative rate constants.
• For blended structures
• In blends, the fill factor a, the maximum open-circuit voltage, V_{oc}, is determined by $HOMO_{donor}$ and $LUMO_{acceptor}$ energy level offsets and further limited by the contact barrier formation. For layers, V_{oc} is increased above this limit due to a substantial diffusion counter-current that is largely absent in blends.nd short-circuit current, J_{SC}, are strongly a function of charge carrier mobility; however, in layers, both quantities saturate with increasing mobility and are more strongly determined by the exciton generation rate near an interface.
• With currently developed materials, power efficiencies greater than 12% should be achievable in blends through graded (rather than homogeneous) morphologies or in layered structures with blended interfaces; however, clean layered structures are limited to significantly lower efficiencies without further improvements in absorption of photons across the solar spectrum.
• Polymer-based photovoltaics, with metal-oxide (TiOx) interlayers, can be manufactured on plastic substrates with all layers being deposited and patterned using low cost liquid-based processing under ambient conditions; however, a reduction in power efficiency up to 50% can result from the lower work function and/or poorer conductivity resulting from the printable metals. Larger area device fabrication favors manufacturing methods such as slot coating and gravure over screen printing.
• Polymer devices using metal-oxide (i.e. TiOx) interlayers are considerably more stable than structures based utilizing doped-polymer (i.e. PEDOT-PSS) interlayers.
• Morphology (including thickness) is critical in all aspects of device performance, from deactivation of the excited state to charge transport. Poor control over morphology is the critical factor in limiting the power conversion efficiency in polymer-based photovoltaic devices.

High Conversion Efficiency in Polymer Photovoltaics

Device Fabrication
Devices were fabricated inside an inert glove box atmosphere by spin casting the polymer hybrid solution onto a prepatterned ITO on glass or plastic substrate, that has been coated with the appropriate electron and or hole transporting layer, and then evaporating the top electrode. The ITO is either precoated with a titanium oxide sol-gel layer (sintered at 400 C) or a PEDOT-PSS layer, and the evaporated top electrode is either Au or Al, respectively. A flat band diagram for the two structures is shown in Fig. 1 (left side). J-V curves in the dark and under white-light conditions (100 mW/cm^2) were taken inside the glove box. Absorption and steady state PL measurements were taken using Varian and Perkin Elmer spectrometers. Additional steady state and time-resolved PL were taken at NREL.

Materials
For the hole transport layers, a variety of PPV and polythiophene materials were used with different mobilities, band gaps, and crystallinity. Liquid crystalline polymers were synthesized to improve charge mobility, but did not result in improved device performance. In addition,

smaller bandgap polymers that incorporated polythiophene groups into the PPV backbone were synthesized in order to increase the absorption of solar light. This material resulted in similar device performance as their larger bandgap PPV-based counterparts. The overriding factor that dictated the final device performance was the mobility of the hole transport polymer and the choice of the electron transport material. Much of our results used M3EH-PPV (Fig. 1, top middle), a unique derivative of the much more commonly studied MEH-PPV, but with a significantly higher mobility due to increased crystallinity induced by the additional insoluble monomer unit. For the electron transporter, CN-ether-PPV, PCBM (Fig. 1, top middle), TiOx sol-gel and nanoparticles (Fig. 1, right), and PbS nanoparticles (not shown) were studied.

Figure 1: Left: The energy diagrams for two different device architectures studied. In addition, LiF was studied as an interlayer between polymer and aluminum (Al). Middle-top: Structures of some materials used in the studies. Middle-bottom: Relative energy levels of materials. Right: AFM images of TiOx surface made from smooth sol-gel layer and rougher nanoparticle layer.

Device Optimization and Performance

In Figure 2 (right), typical current-voltage (J-V) curves for optimized polymer hybrid blend and layered devices are shown, revealing a more than 3x improvement in J_{sc} over neat M3EH-PPV films on TiO$_2$ and 13x over M3EH-PPV on PEDOT. Polymer-PCBM blends result in a further 4x enhancement. Optimized devices had film thickness ~ 30 ± 5 nm, except for polymer layers for which the best device has at thickness of 20 nm M3EH-PPV/50 nm CN-ether-PPV. Blend performance was optimal at 50% and 80% blend wt% for polymer and PCBM blends, respectively. TiOx devices showed consistently the highest fill factors, with values >60% being observed for some devices at lower light intensities.

Figure 2 (left) shows changes in the short circuit current density, J_{sc}, and fill factor, FF, with blend wt%. For polymer blends, the fill factor is limited by poor transport in CN-ether-PPV due

to the inherent properties of PPV polymers and the presence of the ether linkage that disrupts the conjugation. This effect results in a rapid decrease in the fill factor with increasing CN-ether-PPV percentage that is offset, in part, by the greater exciton dissociation resulting from the blended hybrid structure. Both the fill factor and J_{sc} increase in PCBM as electron transport improves with increased PCBM percentage. The maximum power efficiency observed was typically ~3% for a 1:4 M3EH:PCBM blend. This result was lower than the state-of-art values mainly due to the smaller fill factors observed for M3EH blends compared to the regioregular polythiophene blends. We note that while regioregular polythiophene blends were also fabricated, the results are not included in this study because the materials were found to yield much less consistent results than the PPV-derivatives. Simulations (discussed below) combined with our experimental studies indicate that much higher power efficiencies (>10%) are obtainable for these class of materials by controlling and improving the blend morphology.
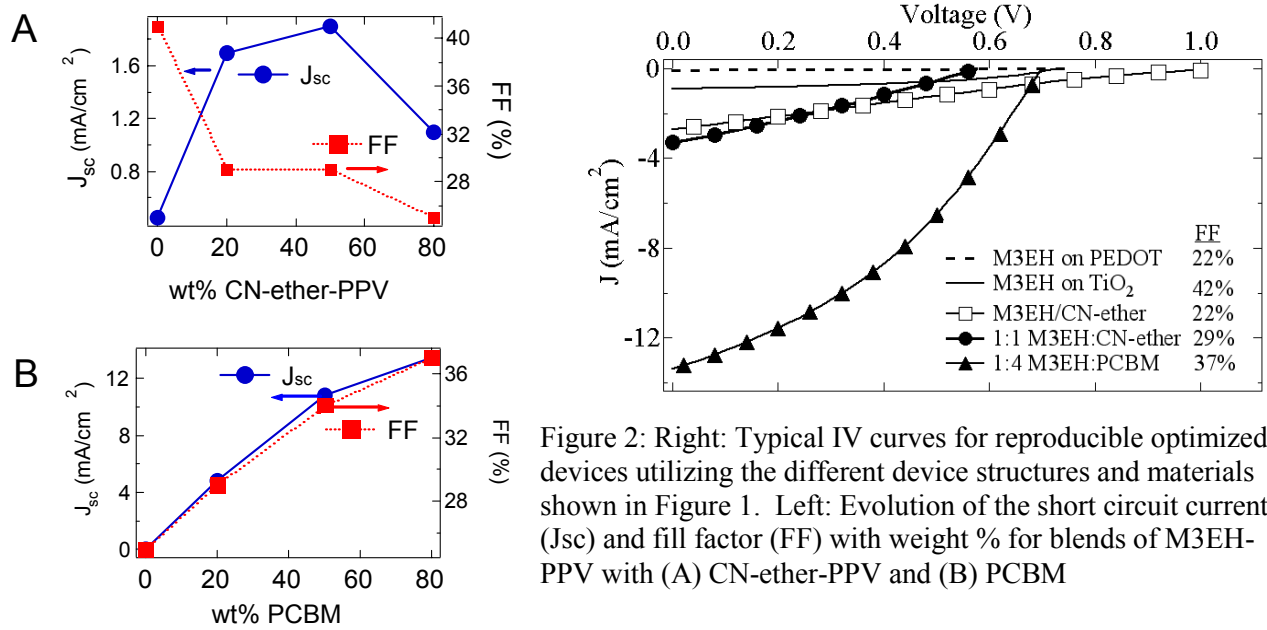
Figure 2: Right: Typical IV curves for reproducible optimized devices utilizing the different device structures and materials shown in Figure 1. Left: Evolution of the short circuit current (Jsc) and fill factor (FF) with weight % for blends of M3EH-PPV with (A) CN-ether-PPV and (B) PCBM

Tandem Devices

In general, device performance was found to be limited by a trade off between photon absorption and charge transport which is optimized by thicker or thinner films, respectively. In an attempt to overcome this limitation, tandem devices consisting of layers of two polymer PV cells were fabricated and studied. Here, challenges were encountered in trying to optimize device performance while maintaining the low cost fabrication by making every layer liquid processible. The liquid deposition of the second PV cell on top of the first PV cell was shown to detrimentally affect its performance, leading to an overall reduction in device performance as the first polymer PV cell was shown to contribute over 75% of the overall power efficiency.

Temperature Dependence of Device Performance

The temperature dependence of the polymer PV were studies from ~100 K to 400 K in order to understand how the device operation and stability were affected by temperature (Figure 3). Since the polymer mobility changes significantly with temperature T (Fig. 3, left) according the formula $\mu \sim \mu^*\exp(-\Delta/kT)\exp(\gamma E^{1/2})$ where Δ is the hopping activation energy γ is the field-prefactor, and E is the electric field across device, these measurements also provide insight on how changes in the polymer's mobility affects device performance. It was found that the short circuit current (I_{sc}) is exponentially dependent on temperature with an activation Δ_{SC} with small

4

variance for a wide range of materials with similar device architectures. Similarly the temperature dependence of the open circuit voltage (V_{oc}) was shown to be largely linear, with the maximum V_{oc} determined by the difference in the HOMO level of the donor, LUMO level of the acceptor, binding energy Φ_B (Fermi Level pinning) and Δ_{SC}. The fill factor increases with increasing mobility as expected. It is noted that device failure tended to occur a few degrees below the glass transition temperature (~300 K to 350 K)) and was worse for devices containing LiF. Temperature-induced device failure was not observed for TiO_x-based devices. The results of the temperature dependent studies for 3 different materials are given in Table 1.

$$Isc(T) = Isc_0 \exp\left(-\frac{\Delta sc}{k_B T}\right)$$

Figure 3: Left: Changes in M3EH-PPV mobility and γ with T. Middle: T-dependence of J_{sc} for PCBM blend (squares), CN-ether-PPV blend (triangles) and a TiOx layered devices (open diamonds), which is described by equation for I_{sc} (left). Right: T-dependence of fill factor and V_{oc} for blends with and without LiF interlayer.
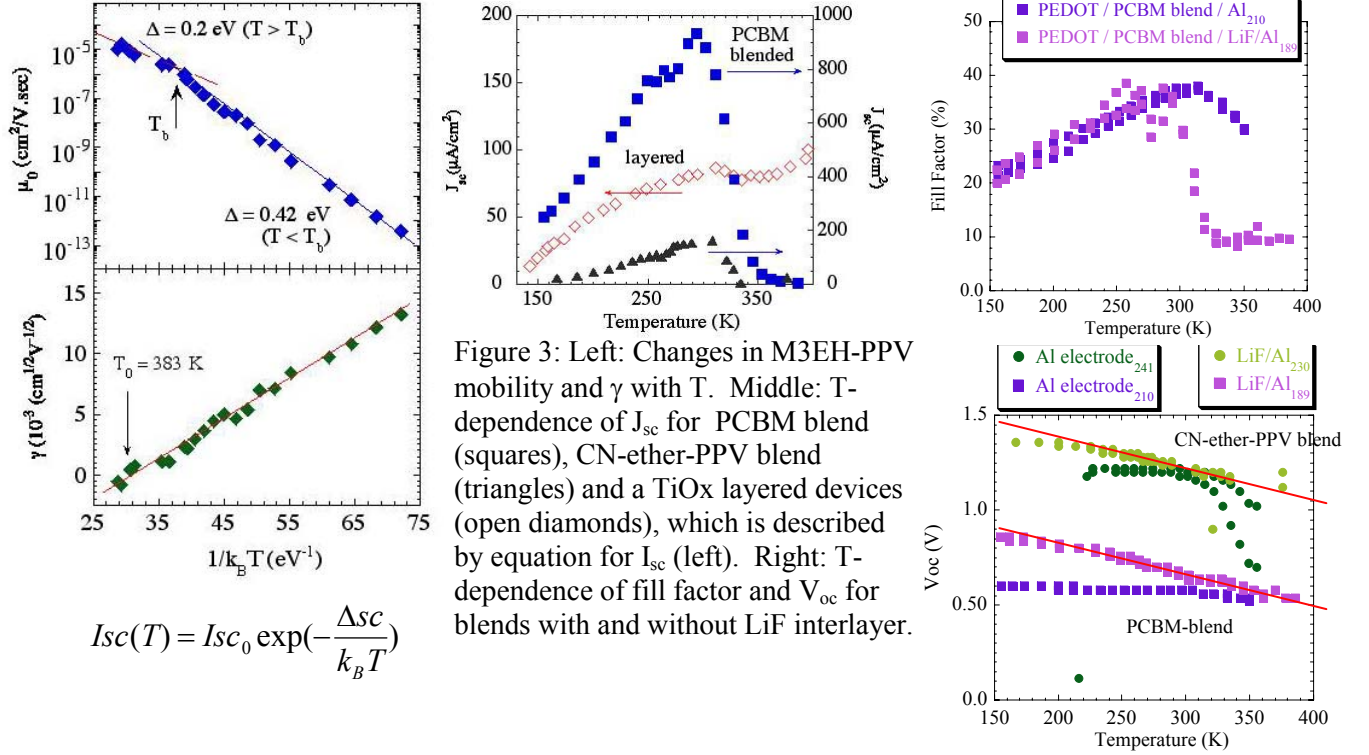
Table 1: Summary of selected results from temperature-dependent studies

Constituent polymer blends	Anode	Δ_{sc}	V_{oc}^*	Δo-Δ_{sc}	Δo-Δ_{sc}-Φ_B
Thio-M3-PPV:PCBM	Al	62 meV	0.95 – 0.0012T (0.6 sat)	1.14	0.68
	LiF/Al	36 meV	1.14 -0.0016T		
M3EH-PPV:CN-ether-PPV	Al	76 meV	(1.22 sat)	1.63	1.27
	LiF/Al	70 meV	1.65-0.0014T (1.36 sat)	1.63	1.36
P3HT:PCBM	Al	75 meV	1.37 – 0.0014T		
	LiF/Al	41 meV			

*Maximum V_{oc} = 1/e(HOMO$_{donor}$ − LUMO$_{acceptor}$-Φ_B) - Δ_{SC} where Δo = HOMO$_{donor}$ − LUMO$_{acceptor}$

5

Numerical Simulations of Organic PV Devices

A quasi-1D model was developed to model the performance of layered, blended, and partially blended organic PVs which is described in more detail in publications. For blends, a change between phases was allowed at every position throughout the device, and blending at layer interfaces was modeled using mass diffusion into the adjacent layer with 100% being a homogeneous blend. This model enables the determination of device performance as a function of the materials absorption (given index of refraction n & dispersion k), electrode's work function, the organic HOMO and LUMO levels and mobility, the device thickness and material morphology, ambient temperature, and finally the light intensity and spectrum.

As shown in Fig. 4 (top), the short circuit current and power efficiency is a strong function of the blend fraction and mobility, and the best performance is achieved for 67% blend fraction. Layered structures (0%) only obtain a power efficiency of <3% even for high mobility materials due to poor exciton dissociation through the bulk, and homogenous blends are limited to a maximum
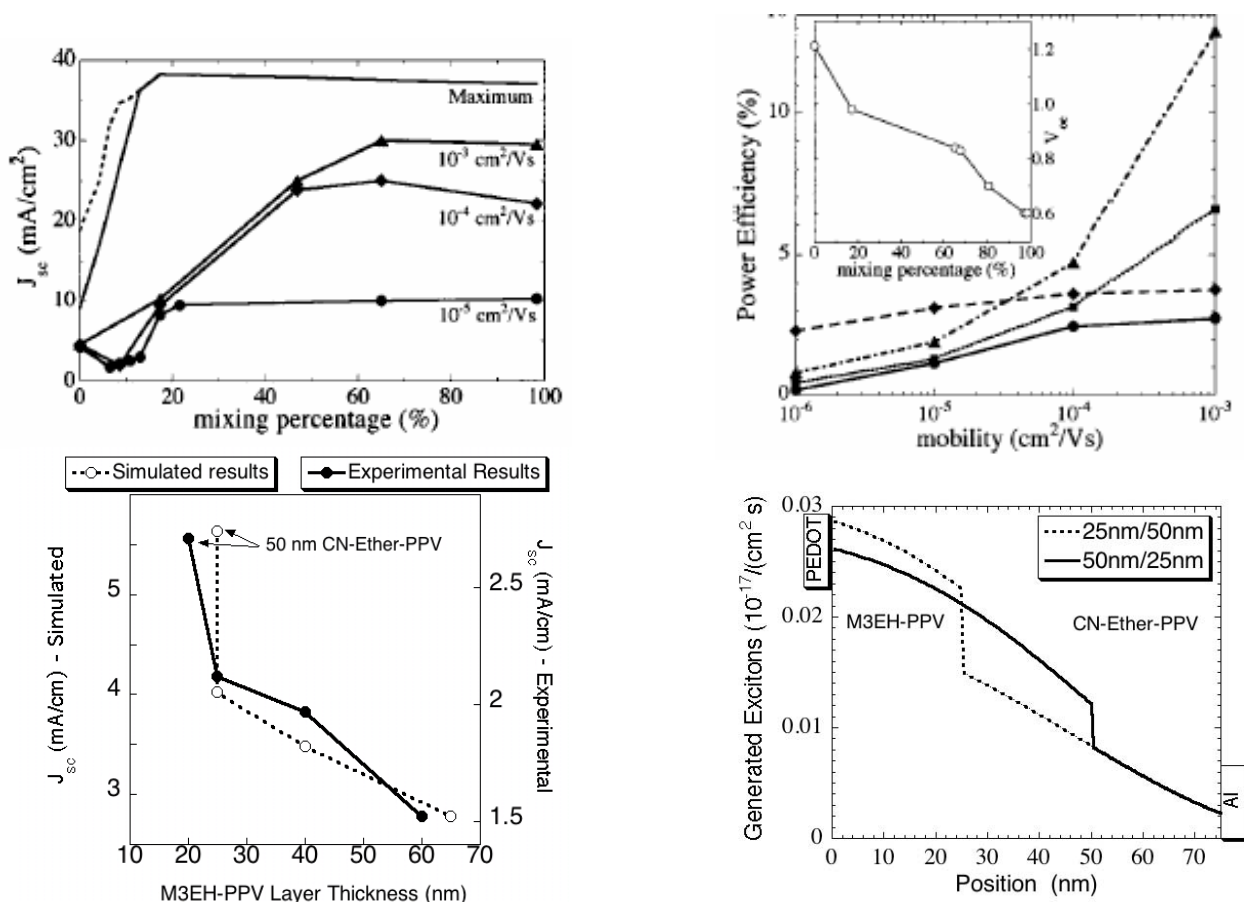
Figure 4: Top: Short circuit current (left) and power efficiency and V_{oc} (right) as a function of blend fraction for polymer/polymer blends. Bottom: Comparison of simulations and experiment for layers (left) and exciton generation rate for two different layer thickness (right) with 25 nm/50 nm resulting in significantly more exciton generation at the polymer interfaces, and ultimately better performance.

power efficiency of ~7.5% due to limits in both charge transport and V_{oc}. The decrease in V_{oc} with increasing blend fraction is due to a decrease in the role of the diffusion counter-current in blends. Higher power efficiencies of ~12% result from partially blended (i.e. graded) structures as these systems optimize exciton generation, dissociation and charge transport. Excellent qualitative agreement between experimental and simulation are obtained for both layers and blends (Fig. 5 left bottom), with quantitative differences due to mobility. Fig. 5 (right bottom) reveals that optical reflection/interference effects can result in large differences in exciton generate rate near interfaces and is a determining factor optimizing the performance of layers.

Additional Research: Steady State and Time Resolved Photoluminescence
The steady state PL was strongly quenched for all layers and blends, with values ranging from 70% for polymer layers to 95% for PCBM/polymer blends. For polymer/polymer systems, the PL and time-resolved data indicate the presence of exciplex formation that can result in exciton scavenging and increased dissociation (Figure 5). For PCBM blends, exciplex formation is not observed; however, a large shift in PL spectrum occurs, due to an effective dilution in the M3EH-PPV at high PCBM wt%.
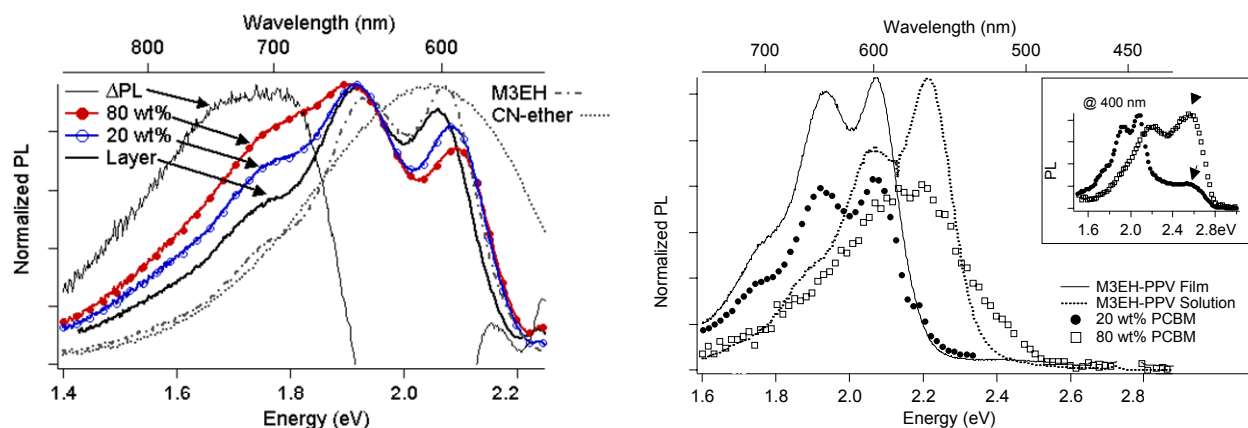
Figure 5: Left: Normalized PL for blend and layered films excited at 540 nm. ΔPL is a subtraction of the M3EH-PPV spectrum from that of the 80% blend, revealing exciplex formation in polymer blends. Right: Normalized PL for PCBM blends.

Time Resolved Photoluminescence
In the left part of Figure 6, the time-resolved PL data for polymer-polymer layers and blends (top) and for PCBM blends (bottom) are shown. In Figure 6 (right) and Table 2, the decay times for the pristine polymers as well as the blended and layered structures are summarized. All blends and layers show a very rapid decay time (<0.05 ns). For polymer blended structures, significant exciton quenching occurs in both the electron- and hole-transporting polymers due to the interpenetrating morphology; however, the lack of complete quenching limits the achievable short-circuit currents. In layered structures, decay times were longer than for blends; thus exciton dissociation and charge transfer is more efficient in blended than in layered devices. Both steady-state and time-resolved data indicate that charge transfer occurs to an intermediate exciplex state in blended and layered structures of CN-ether-PPV with M3EH-PPV. The exciplex is characterized by a decay component of ~ 2.0 ns which predominates at 700 nm emission – the location of a broad, featureless steady-state spectral feature attributed to exciplex emission. Formation of the exciplex aids device performance, as indicated by the predominance

of the exciplex peak (and notable absence of M3EH-PPV emission) in steady-state spectroscopy on particularly efficient photovoltaic devices. The exciplex may thermally re-excite the M3EH-PPV exciton, providing an additional route for charge separation, or dissociate directly under the influence of an electric field.

Photoluminescence decay from PCBM aggregates is detected in all heterojunctions. Decay from the PCBM phase is characterized by a time constant of 1.0 - 1.9 ns (see Table 2). PCBM quenches the excited state more efficiently than CN-ether-PPV, but the dominant decay time of M3EH-PPV (0.20 ns) is only ~75% for both systems, indicating incomplete quenching. Contrary to the naïve assumption that more PCBM should result in increased charge transfer (shortening the lifetime), the rate of decay *increases* as the wt% of PCBM in the blend is *decreased*, counter to the enhanced device performance at high wt% of PCBM in the blend (Table 2). These results indicate the importance of charge transport over exciton dissociation , on device performance.
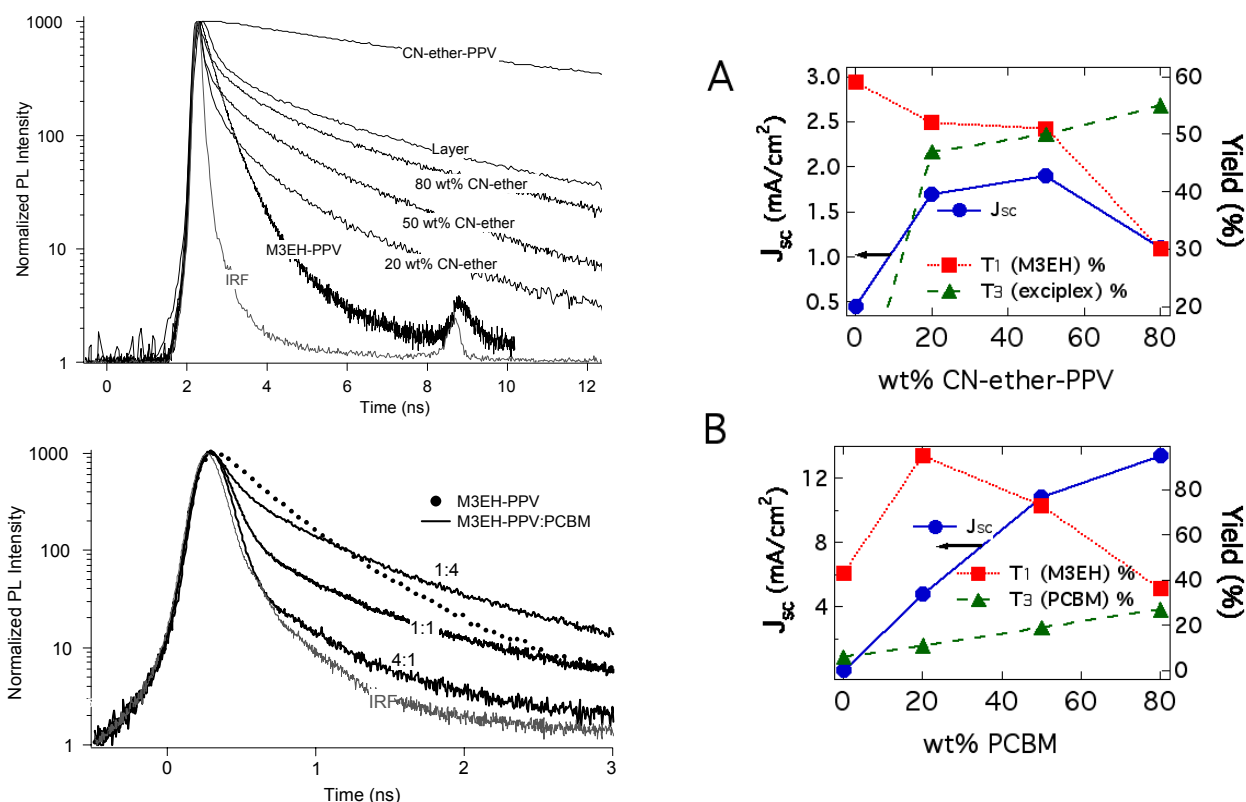
Figure 6: Left: Time-resolved PL data for polymer-polymer layers and blends (top) and for PCBM blends (bottom). Note that all the layers and blends exhibit an initial faster decay than the neat M3EH-PPV film although the average decay time is longer (except for 20 wt% PCBM blend). The CN-ether-PPV decay components are readily quenched, but the ~0.45 ns M3EH-PPV decay remains for all material combinations (see Table 2). Right: Summary of the yield of the major decay components (M3EH-PPV, PCBM, and exciplex) as a function of the CN-ether-PPV wt % (top) and the PCBM wt % (bottom).

Table 2: Summary of decay times of CN-ether-PPV and PCBM blends compared to neat film results.

	Film	η	τ_1 (ns)	τ_2 (ns)	τ_3 (ns)	τ_{ave} (ns)	Q
Pristine polymers	M3EH-PPV	0.04%	0.20 (43%)	**0.45 (53%)**	1.7 (3%)	0.38	
	CN-ether-PPV	N/A	0.30 (2%)	4.3 (26%)	**12.2 (73%)**	10.0	
CN-ether blends	50 wt% CN-ether w/ M3EH-PPV	0.86%	**0.05 (51%)**	0.46 (20%)	2.0 (22%)	1.0	75%
	M3EH/CN-ether layer	0.89%	**0.05 (39%)**	0.46 (17%)	2.0 (27%)	1.8	75%
TiOx layer	TiOx/M3EH-PPV	0.5%	0.12 (42%)	**0.32 (44%)**		0.35	0%
PCBM blends	80 wt% PCBM w/ M3EH-PPV	3%	0.05 (36%)	**0.50 (49%)**	1.9 (16%)	0.6	75%
	20 wt% PCBM w/ M3EH-PPV	0.9%	**0.02 (95%)**		1.0 (5%)	0.07	90%

New Materials for Luminescent Solar Concentrators

The use of Luminescent Solar Concentrators (LSC) to generate electricity from solar radiation was introduced around 30 years ago and was based on earlier work that used fluorescence radiation converters as an inexpensive method to detect scintillation light over large areas. A LSC uses a photoluminescent material to absorb the suns photons, remit these photons at longer wavelengths, waveguide the emitted photons down a large area waveguide structure, and then convert the longer wavelength photons to electricity using strips of silicon-based photodetectors. The advantage of this technology is that one can use very inexpensive materials, usually organic dyes imbedded in a polymer matrix, to absorb the solar light and concentrate it; therefore, a much smaller area of the expensive silicon PV is needed. The device performance, however, was found to be severely limited by self absorption of the emitted light, absorption over solar spectrum and the dye efficiency; the highest power efficiencies obtained on the a LSC was reported in 1985 to be 4% using a two-stack concentrator and a relatively expensive GaAs solar cells. Since then, quantum dots have been discussed as new LSC's and one group has started field testing organic LSCs although the power efficiencies are still too low for viable commercialization.

The power efficiency of a LSC cell is determined by the following formula:

$\eta_{LSC} = \eta_{PL} * \eta_{abs} * \eta_{WG} * \eta_{Si}$

where η_{PL} is the edge photoluminescence efficiency (includes self absorption), η_{abs} is the fraction of the solar spectrum absorbed, η_{WG} is the fraction of light that is waveguided, and η_{Si} is the power efficiency of the silicon detector at the wavelength of the emitted light. To achieve a solar power efficiency grater than 10% using standard silicon detectors, the luminescent material should have a η_{PL} >90%, and a η_{abs} >67% with minimal self absorption. Our group at UCSC has identified a small molecule dye with sufficient Stokes-shift to minimize self-absorption and solar absorption, as shown in Figure 7; however, its η_{PL} is on the order of 20%. Conversely, a

conjugated red-emitting polyfluorene material has also been identified that has a high η_{PL} (>90%); however, the absorption across the visible and Stoke's shift is too limited. The η_{PL} of the small molecule dye can be increased by using surface enhanced fluorescence effects and/or surfactants, and the absorption across the visible (and Stoke's shift) for the semiconducting polymer-based system can be improved through the incorporation if IR-emitting organic chromophores or inorganic quantum dots. This research has now obtained funding from the PIER program administered by the CEC and the State of California.

Figure 7: Top: Normalized absorption (abs) and light emission (rad) for an organic laser dye (LDS821) and a light emitting polymer (Red PF), overlayed with Si's EQE. Bottom: Typical design for a LSC.
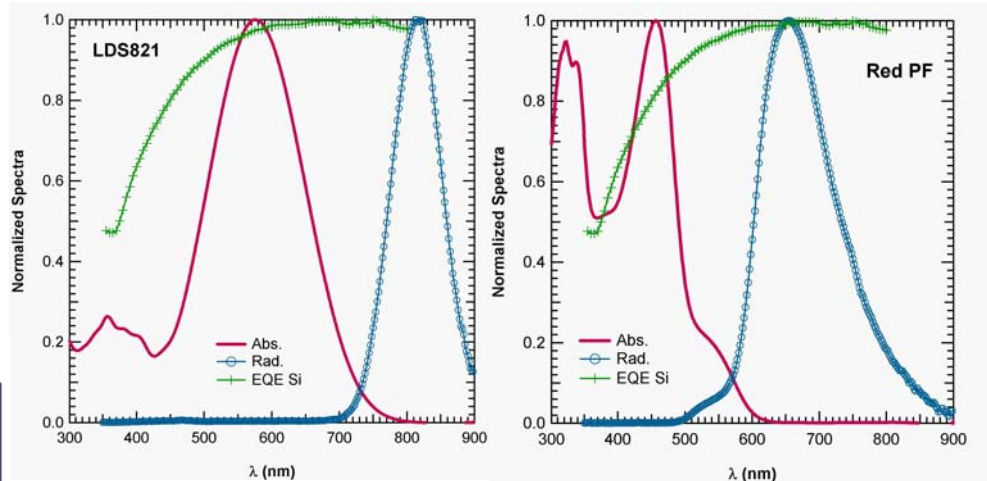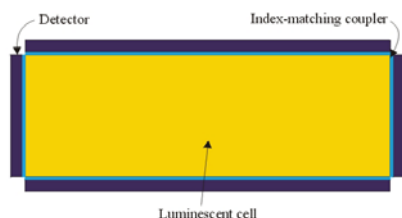
Long Lifetime and Reliability With an Inexpensive Manufacturing Process

Inexpensive Manufacturing Process
Devices were constructed on PET plastic substrates (Vitex) to compare with devices manufactured on glass (Figure 8, top). The power efficiency is reduced less than 10% from cells made on glass substrates. Methods were also investigated to make a fully printable solar cell under atmospheric conditions by eliminating the need for an evaporated top electrode. Because materials with work function similar to Al are not printable, full printability is only achievable with the TiO_x layered structures. Two printable electrodes were studied: a solvent soluble silver paste and a water soluble conducting polymer, PEDOT-PSS. Working devices were fabricated using both of these top electrodes although the silver has a lower open circuit voltage due to its lower work function than PEDOT-PSS and Au (Figure 8, bottom). The power efficiency is normally reduced by a factor of 50% or more from those cells made with an evaporated top Au electrode. Large areas devices (>50 cm^2) were also fabricated using a complete printing process in collaboration with Add-vision. Using this process, the thin larger areas devices had difficulties with shorting and the thick devices suffered from low power efficiency. New methods to
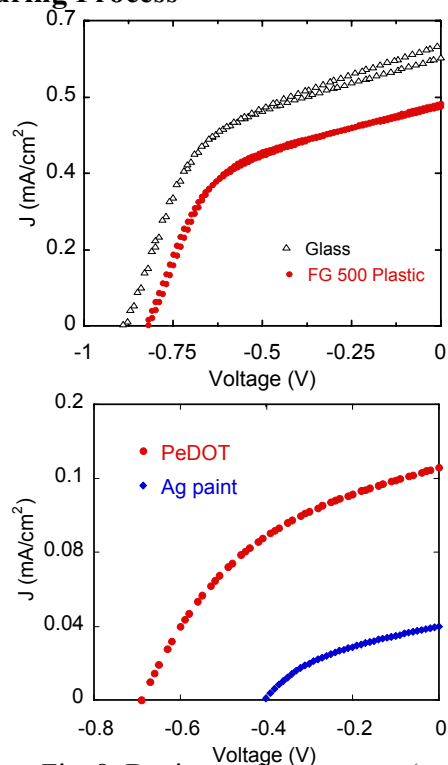

Fig. 8: Device performance on (top) plastic & (bottom) of printed contact.

10

liquid deposit smooth larger area solar cells and to improve the overall power efficiency of these inexpensive devices are now being developed under an NSF STTR Phase I grant.

Lifetime Properties of Device Structures

Lifetime behavior of all three types of devices (polymer blends, TiOx layers, and PCBM blends) was monitored for changes in their IV-curves and quantum efficiency upon exposure to solar radiation. The blended devices were observed to degrade the fastest (typically <30 days), with PCBM blends being the most unstable, while the TiOx layers were stable for the duration of the test (>80 days). The rapid degradation of the blends appeared to be caused by UV-induced damage to the PEDOT-PSS and PPV polymers that was mitigated by including TiOx in the device structure. The rapid degradation of the PCBM blend devices were also observed for devices kept in a dark dry nitrogen atmosphere. The significantly short shelf life (7 days) of PCBM blend (Figure 9, top) was likely due to the chemical change in PCBM itself or a chemical reaction with PCBM. In those 7 days, the Isc decreased by 60 % while the V_{oc} remained constant. In contrast, the TiOx devices showed shelf life of over one year (Figure 9, bottom). The V_{oc} and FF both increased while I_{sc} remained constant. The largest increase in V_{oc} occurred within the first 30-60 days, and eventually reached ~0.8 V. This is due to the evolution of Au-polymer interface. The interface between the soft gold and polymer surface heals over a period of time due to slow diffusion, resulting in a better ohmic contact. In contrast, Al and printed electrodes appear to form a good initial contact upon deposition.
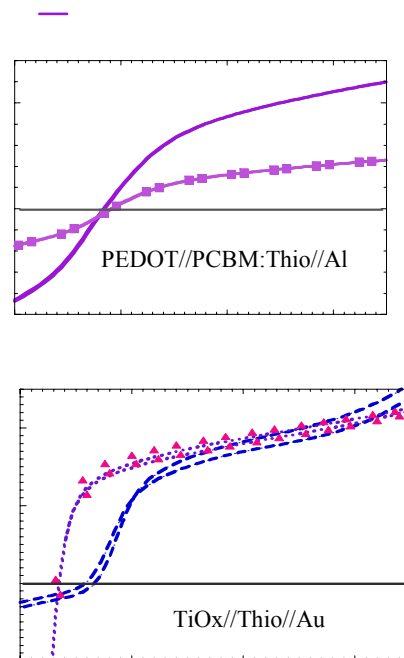

Fig. 9: Shelf-life of PV cells

Papers in Scientific Journals

1. Improving Power Efficiencies in Polymer - Polymer Blend Photovoltaics. A. J. Breeze; Z. Schlesinger; S.A. Carter; H. -H. Hoerhold; H. Tillmann, Solar Energy Mater. and Solar Cells 83, 263-271 (2004).
2. Numerical Simulations of Layered and Blended Organic Photovoltaic Cells, J. O. Haerter, S.V Chasteen, S. A. Carter, J. C. Scott, Applied Physics Letters (86), 164101 (2005).
3. Exciton Dynamics and Device Performance in Polythiophene Heterojunctions for Photovoltaics. S. V. Chasteen, S. A. Carter, G. Rumbles, Proc. of SPIE (5938), 59380J-1, 2005.
4. Blended versus Layered Structures in Polymer Photovoltaics. S. V. Chasteen, J. O. Haerter, G. Rumbles, C. Scott, S. A. Carter. J. of Applied Physics, March, 2006.
5. The effect of ether-linkage upon photophysics and dynamics in PPV polymers: CN-PPV vs. CN-ether-PPV, S. V. Chasteen[1], G. Rumbles[2], S.A. Carter, J. of Chem. Phys. (in press).
6. Towards optimization of device performance in conjugated polymer photovoltaics: Charge generation and transport in poly (p-phenylene vinylene) polymer heterojunctions, S. V. Chasteen, V. Sholin, S. A. Carter and G. Rumbles (in final preparation).
7. Temperature Dependence of Polymer Photovoltaic Devices, Y. K. Nakazawa and S. A. Carter, H. H. Hoerhold, Applied Physics Letters (in review).

* Also Sue Carter was general editor of Materials Research Society Bulletin 2005 responsible for Theme Issue on Organic Photovoltaics

Papers in Popular Press
1. Bonnie Raitt powers solar benefit By STEPHANIE CHASTEEN, November 15, 2002, 03local.htm, Search in: 2002 Archives
http://www.santa-cruz.com/archive/2002/November/15/local/stories/03local.htm
2. Solar-energy research heats up By STEPHANIE CHASTEEN, November 10, 2002 02local.htm, Search in: 2002 Archives
http://www.santa-cruz.com/archive/2002/November/10/local/stories/02local.htm
3. Solar power still too expensive By STEPHANIE CHASTEEN, November 10, 2002 06biz.htm, Search in: 2002 Archives
http://www.santa-cruz.com/archive/2002/November/10/biz/stories/06biz.htm

Ph.D. Thesis

1. Yuko Nakazawa, "Temperature Dependent Studies of Polymer Photovoltaics," December 2004.
2. Stephanie Chasteen, "Excited State Dynamics in Polymer Photovoltaics," December 2005.

Presentations of results from this contract

Invited Talks
1.Melissa Kreger, SPIE symposia on Organic Photovoltaics, Seattle, July 2002.
2. Melissa Kreger, American Chemical Society Meeting, Boston, August 2002
3. Sue Carter, Colloquia at the University of California, Davis, Spring 2003.
4. Sue Carter, Colloquia at the Naval Postgraduate School in Monterey, May 2004.
5. Sue Carter, Hallgren Lecturer at General Electric, GE, May 2004.
6. Sue Carter, Platts E Source Energy Conference, Colorado Springs, 2004
7. Sue Carter, SPIE symposia on Organic Photovoltaics, August, 2004
8. Sue Carter, American Chemical Society Meeting, San Diego, 2005.
9. Sue Carter, Materials Research Society, Spring Meeting, San Francisco, 2006.

Contributed Talks
1. Melissa Kreger, Talk at MRS symposia on Organic Electronics, San Francisco, April 2002.
2. Yuko Nakazawa, MRS symposia on Materials for Renewable Energy, December, 2004.
3. Jan Haerter, American Physical Society, LA, March 2005.
4. Stephanie Chasteen American Physical Society, LA, March 2005
5. Yuko Nakazawa, American Physical Society, LA, March 2005.
6. Sue Carter, IEEE World Conference on Photovoltaic Energy Conversion, May, 2006.

Conference Posters
1. Tosan Ombegeho, MRS symposia on Organic Electronics, San Francisco, April 2002.
2. Yuko Nakazawa, MRS symposia on Organic Electronics, April 2002.
3. Stephanie Chasteen, MRS symposia on Organic Electronics, April 2002.
4. Yuko Nakazawa, SPIE symposia on Organic Photovoltaics, Seattle, July 2002.
5. Stephanie Chasteen, SPIE symposia on Organic Photovoltaics, Seattle, July 2002.

REPORT DOCUMENTATION PAGE		Form Approved OMB No. 0704-0188

1. **REPORT DATE** *(DD-MM-YYYY)* July 2006	2. **REPORT TYPE** Subcontract Report	3. **DATES COVERED** *(From - To)* 1 September 2001 – 30 April 2006

4. TITLE AND SUBTITLE
Polymer Hybrid Photovoltaics for Inexpensive Electricity Generation: Final Technical Report, 1 September 2001 – 30 April 2006

5a. CONTRACT NUMBER
DE-AC36-99-GO10337

5b. GRANT NUMBER

5c. PROGRAM ELEMENT NUMBER

6. AUTHOR(S)
S.A. Carter

5d. PROJECT NUMBER
NREL/SR-520-40044

5e. TASK NUMBER
PVA60001

5f. WORK UNIT NUMBER

7. PERFORMING ORGANIZATION NAME(S) AND ADDRESS(ES)
University of California, Santa Cruz
Santa Cruz, CA 95064

8. PERFORMING ORGANIZATION REPORT NUMBER
ACQ-1-30619-03

9. SPONSORING/MONITORING AGENCY NAME(S) AND ADDRESS(ES)
National Renewable Energy Laboratory
1617 Cole Blvd.
Golden, CO 80401-3393

10. SPONSOR/MONITOR'S ACRONYM(S)
NREL

11. SPONSORING/MONITORING AGENCY REPORT NUMBER
NREL/SR-520-40044

12. DISTRIBUTION AVAILABILITY STATEMENT
National Technical Information Service
U.S. Department of Commerce
5285 Port Royal Road
Springfield, VA 22161

13. SUPPLEMENTARY NOTES
NREL Technical Monitors: R. McConnell, F. Posey-Eddy

14. ABSTRACT *(Maximum 200 Words)*
The project goal is to understand the operating mechanisms underlying the performance of polymer hybrid photovoltaics to enable the development of a photovoltaic with a maximum power conversion efficiency over cost ratio that is significantly greater than current PV technologies. Plastic or polymer-based photovoltaics can have significant cost advantages over conventional technologies in that they are compatible with liquid-based plastic processing and can be assembled onto plastic under atmospheric conditions (ambient temperature and pressure) using standard printing technologies, such as reel-to-reel and screen printing. Moreover, polymer-based PVs are lightweight, flexible, and largely unbreakable, which make shipping, installation, and maintenance simpler. Furthermore, a numerical simulation program was developed (in collaboration with IBM) to fully simulate the performance of multicomponent polymer photovoltaic devices, and a manufacturing method was developed (in collaboration with Add-vision) to inexpensively manufacture larger-area devices.

15. SUBJECT TERMS
PV; polymer hybrid photovoltaics; cost; inexpensive manufacturing process; conversion efficiency; device; large-area; plastic; printing technologies; numerical simulation

16. SECURITY CLASSIFICATION OF:			17. LIMITATION OF ABSTRACT	18. NUMBER OF PAGES	19a. NAME OF RESPONSIBLE PERSON
a. REPORT Unclassified	b. ABSTRACT Unclassified	c. THIS PAGE Unclassified	UL		19b. TELEPONE NUMBER *(Include area code)*

Standard Form 298 (Rev. 8/98)
Prescribed by ANSI Std. Z39.18